

Effect of uncertainty on load position in the fatigue life of steel-fiber reinforced concrete under compression

Manuel Tarifa  · Gonzalo Ruiz  · Elisa Poveda  · Xiaoxin Zhang  · Miguel A. Vicente  · Dorys C. González 

Received: 19 July 2017 / Accepted: 29 January 2018 / Published online: 3 February 2018
© RILEM 2018

Abstract The high scatter of the compressive fatigue life of concrete and fiber reinforced concrete, which may normally reach two orders of magnitude, is caused not only by material heterogeneity, but also by the random nature of the unwanted eccentricity during the tests. It mainly arises from misalignments due to manual specimen centering, although tolerances in experimental equipment and in the geometry of the specimens may cause eccentricity too. In order to minimize it, an individualized ball-and-socket joint (i-BSJ) was designed for this research. An instrumented aluminum cube was used to characterize the probabilistic distribution of the undesired eccentricity under two testing conditions, that is, with and without the i-BSJ. The standard deviation of the loading eccentricity was one order of magnitude smaller with the new device. Secondly, two series of 15 compressive tests and two series of 15 fatigue tests were performed

on 40 mm edge-length steel-fiber reinforced concrete cubes, again with and without the special device. The fatigue series range from 24 to 88% and from 36 to 82% of their respective compressive strength, f_c . The use of the i-BSJ produced an increase of 10% in the average f_c while its standard deviation decreased by 40%. Similarly, the average fatigue life tripled for the first series and was six times longer for the second series, notwithstanding the loading limits in the low-eccentricity series referring to the enhanced f_c . Correspondingly, the standard deviation of the number of cycles until failure decreased by 50% in the two fatigue series performed with the i-BSJ.

Keywords Undesired eccentricity minimization · Reduction of scatter on fatigue results · Enhancement of concrete fatigue life · Fatigue of steel-fiber reinforced concrete

M. Tarifa
E.I. Minera e Industrial de Almadén, Universidad de Castilla-La Mancha, Pza. Manuel Meca 1,
13400 Almadén, Spain

G. Ruiz (✉) · E. Poveda · X. Zhang
E.T.S. de Ingenieros de Caminos, C. y P., Universidad de Castilla-La Mancha, Avda. Camilo José Cela s/n,
13071 Ciudad Real, Spain
e-mail: Gonzalo.Ruiz@uclm.es

M. A. Vicente · D. C. González
E. Politécnica Superior, Universidad de Burgos, Campus Milanera. C/ Villadiego s/n, 09001 Burgos, Spain

1 Introduction

Compressive fatigue tests on concrete specimens are usually performed by means of servo-hydraulic testing machines. These machines are normally equipped with a spherical seat in order to protect the load cell and the actuator from damaging eccentric loads. Compressive tests should be performed under centered axial load, which is indirectly stated in the codes by

prescribing the use of a spherical seat attached to the upper platen and by recommending a careful centering of the specimen [1]. However, it is not common to use a technique to minimize the eccentricity other than the ability of the operator to align the specimen. This, together with geometric tolerances in experimental equipment and in the geometry of the specimens, may result in axial misalignments. Even so, the effect of undesired random eccentricity on compressive strength is considered to be small whereas, when measuring the elastic modulus, it is usually prescribed to average axial strains at axisymmetric generatrices to compensate for loading eccentricity [2].

On the other hand, it is generally accepted that fatigue tests on concrete exhibit a large scatter in the number of cycles to failure [3–6], and it may reach up to three orders of magnitude. For instance, this can be appreciated in a summary of a large number of experimental results by Susmel [5], which contain fatigue results of plain concretes and short-fiber/particle reinforced concretes subjected to uniaxial cyclic loading. Due to the substantial scatter in test results, a statistical evaluation of fatigue experiments is mandatory [3], which leads either to formulating fatigue models, accounting explicitly for failure probability [7, 8] or introducing high safety coefficients to assess the uncertainty in fatigue prescriptions within construction codes [9, 10].

The fatigue behavior of concrete began to be studied in the 1930s. Since then, numerous experiments have been conducted to study the influence of different fatigue parameters [11–19] on fatigue life N (number of cycles resisted before failure). In particular, Aas-Jakobsen [20] studied the effect of the stress ratio R , which is the relationship between σ_{\min} and σ_{\max} , on fatigue life. Tepfers and Kutti [21] and Tepfers [22] confirmed the results years later. The influence of the loading frequency on fatigue life has been also studied from the 1930s by Graf [11, 12], and presently by Medeiros et al. [19]. On the other hand, other effects on fatigue behavior, regarding the material composition, have been studied. Thus, the effect of moisture conditions on normal strength concrete was studied by Hilsdorf and Müller [23], and the influence of high performance strength concrete on fatigue life was studied by Waagaard et al. [24] and by Petkovic et al. [25].

Regarding scatter, Holmen [26] pointed out that most of it can be explained by the variability of the

static concrete strength, which is also supported by Siemes [27] for plain concrete and Cachim et al. [28] for fiber reinforced concrete. On the other hand, monotonic compressive tests can be considered a limit case of compressive fatigue tests [7], where the failure is reached in only one cycle. In addition, while monotonic tests follow specific standards, as the ASTM C39 [1] (which is analogous to EN 12390-3 [29]), concrete fatigue tests are only guided by recommendations that assume that the same experimental set-up, as in monotonic tests, is going to be used [3, 4]. Moreover, it is generally accepted that a certain scatter in the fatigue of concrete results must be tolerated and reliability methods must be used to accommodate it. Maybe this is the reason there is scarce research on the actual causes of scatter and on the possibility of reducing it. Concrete heterogeneity, specially micro-cracks and voids, should be responsible for some of the scatter, but it is likely that another part of it can stem from tests assumptions that are not actually considered, such as having centered loads in uniaxial tests.

In this respect, it seems apparent that eccentric loads in compression should have a deleterious effect on fatigue life. However, the authors of CEB 188 [3], which is a state-of-the-art authority on concrete fatigue, affirm that the stress gradient caused by eccentric loading is a causative factor of fatigue life enhancement. The statement is based on the results by Ople and Hulsbos [30], who indeed reported that fatigue life with stress gradients was longer than with uniaxial loads, but it was so provided the maximum strain in the most-loaded fiber was the same. This is a condition that is not mentioned by CEB 188 (incidentally, ACI 215 [4] also cites these results, but does report the quoted experimental condition). Likewise, Mindess et al. [31], in their general book on concrete, state that stress gradients have a significant effect on fatigue life and lead to fatigue strengths approximately 15% higher than those obtained from similar specimens loaded uniformly. Once again, this comment may arise from an inaccurate interpretation of the results in [30] through CEB 188 [3]. It is also likely that Mindess et al. [31] account for some type of redistribution in flexural specimens, especially in the presence of confinement due to reinforcing rebars. In fact, this stress redistribution is considered by Zanuy et al. [6]. In any case, it should be noted that it is not the effect of eccentric loads on concrete



fatigue which this paper addresses, but the impact of uncertainty in regard to load position, i. e. the effect of the probabilistic distribution of unwanted eccentricity on fatigue results.

Therefore, this research is aimed at determining the effect of uncertainty on load position in fatigue life and its scatter on concrete compressive tests. Actually, a steel-fiber reinforced concrete (SFRC) was chosen to achieve larger levels of scatter rather than plain concrete [28, 32]. Thus, cyclic tests were performed on SFRC cubes in order to obtain the experimental fatigue life and its scatter, produced by the ability of the operator to align the specimens in the testing machine. Furthermore, the normal density function of experimental eccentricity was characterized by an instrumented aluminum specimen. In addition, a corrective measure was taken by means of the design of an individualized ball-and-socket joint (i-BSJ) which had the same size as the specimen surface, and which led the eccentricity to decrease and the fatigue life to increase thereby showing less scatter.

The rest of the paper is structured as follows: The experimental procedure is presented in the next Section, which is followed by the description of the results of the tests. Finally, the conclusions are drawn in the last Section.

2 Experimental procedure

Materials and tests aimed at determining the influence of the uncertainty on load position in fatigue life are described in this section. In addition, the design of an individualized ball-and-socket joint (i-BSJ) to minimize loading eccentricity is also described.

2.1 Materials and specimens

Cubic specimens from a single self-compacting concrete, reinforced with steel-fibers, were used throughout the experiments. The self-compacting concrete matrix was made of a siliceous aggregate of a maximum size of 8 mm and CEM I 52.5 SR cement. The mixing proportions by weight were 1:0.32:2.25:1.73:0.44:0.012 (cement:filler:sand:coarse aggregate:water:superplasticizer). The dosage of steel fibers was 15 kg/m³ of BEKAERT OL 13/0.2, which are 13 mm in length and 0.20 mm in diameter,

resulting an aspect ratio of 65. Their tensile strength was 2600 MPa. This fiber reinforcement was not expected to influence the quasi-static strength of the plain material [32, 34], but rather to increase the scatter of the number of cycles to failure in fatigue tests [28, 32]. Moreover, as the mix was self-compacting (the value of the slump flow test was 67 cm and the time to reach a diameter of 50 cm or T500 was 1.50 s), fiber segregation was avoided [33].

The cubes were 40 mm in edge-length with a tolerance of ± 0.2 mm. They were cut from prisms of 100×100 mm² in cross-section and 420 mm in length. Specifically, prisms were cut into nine slices, each slice was cut into two small prisms and from each of them, again by cutting, two cubes were obtained. All the faces of these cubes were ground to the prescribed dimensions, accounting for the aforementioned tolerance. This process was performed so that the cubes were obtained from the core of the original prism, thus avoiding the ‘wall effect’, i. e. preferential fiber alignment and concentration near the specimen outer faces in contact with the mould [34]. A total of 90 cubes were used in this research.

All the tests were performed with a servo-hydraulic Instron machine, capable of applying 250 kN of load, equipped with a spherical seat, a Instron T1086-63 model with a diameter of 95 mm, for ensuring that the loading axis coincides with the axis of the actuator and the load cell, see Fig. 1. In order to minimize the influence of misalignments due to manual specimen

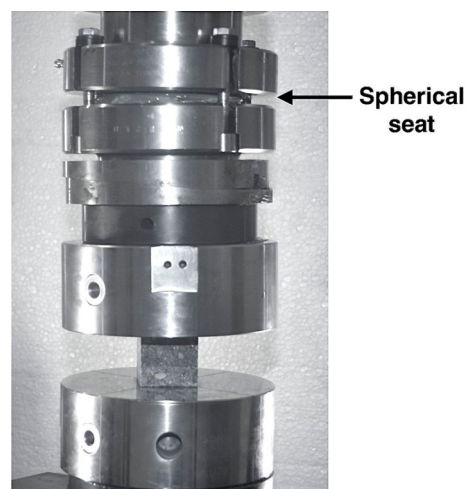


Fig. 1 Servo-hydraulic Instron machine equipped with a spherical seat

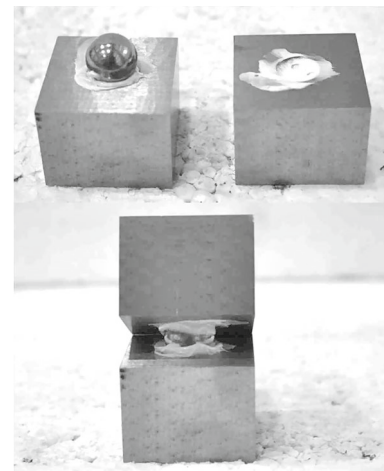
centering, we made marks in the platen surface to indicate the correct theoretical position. Careful manual alignment with the help of marks was followed by adjusting the spherical seat at a pre-load of 2 kN prior to the start of each test. Moreover, this alignment process was always performed by the same person in all the tests described herein. It should also be noted that cubes were tested as they were cast, i. e. the loading axis always coincided with the vertical direction during casting.

2.2 Design of an individualized ball-and-socket joint

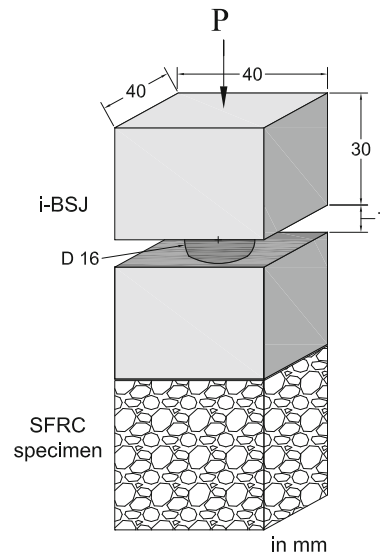
A special device was designed in order to minimize the undesired loading eccentricity on specimens due to specimen centering. It was composed of two square steel platens with the same cross-section as the cubic specimens to be tested, $40 \times 40 \text{ mm}^2$, and 30 mm in height. A round ball of 16 mm in diameter was placed between the two steel platens into two spherical recesses of 4.5 mm in depth, in order for there to be a space of 7 mm between the two platens. The recesses were lubricated to allow free rotation. Thus, the set functioned as an individualized ball-and-socket joint (i-BSJ), see Fig. 2.

2.3 Tests to characterize the load eccentricity

The load eccentricity on a specimen depends on its geometry, the geometrical details of the spherical seat of the machine and the specimen positioning between the steel platens of the machine. High scatter on the fatigue life of small specimens would be expected due to the difficulty of correctly aligning them with the loading axis of the testing machine. Thus, in order to characterize the actual eccentricity, compressive tests on an instrumented aluminum cubic specimen of 40 mm in edge-length, were performed. The specimen was manufactured with a tolerance of $\pm 0.1 \text{ mm}$. It was instrumented with four strain gauges bonded in the middle of the four free faces, parallel to the application of the load, see Figs. 3 and 4. The strain gauges used were HBM type 6/120ALY11, 6 mm in length and 2.8 mm in width, with a resistance of 120Ω and a transverse sensitivity of 0.1%. The bonded strain gauges were referred to as SG (strain gauge), followed



(a)



(b)

Fig. 2 Components (a) and dimensions (b) of the individualized ball-and-socket joint (i-BSJ)

by a number indicating the face of the cube it was attached to.

These characterization tests were performed at a loading rate of 0.3 MPa/s until 110 MPa, following the alignment procedure mentioned above. It is noteworthy that after each test, the aluminum cube was removed from the machine steel platens in order to start the alignment procedure from scratch with each fresh test. A total of thirty characterization tests were performed, fifteen with the use of the i-BSJ and another fifteen without it. The stress-strain curves at

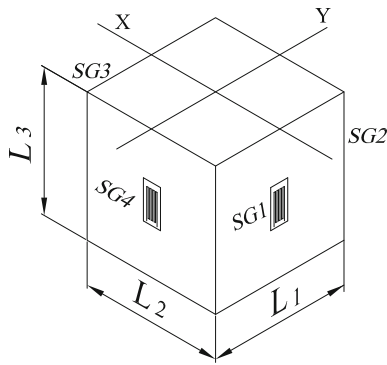


Fig. 3 Strain gauges bonded on the aluminum cube and coordinate system



Fig. 4 Instrumented aluminum cube, with the i-BSJ, between the machine steel platens

the center of all the free sides of the cube were measured during each test.

These strains were employed to calculate the normal two-dimensional density function of the load eccentricity with reference to an orthogonal coordinate system, which originally was placed at the center of the mass of the cube, see Fig. 3. To do so, an assumption of a linear elastic material, frictionless contact between the specimen and the machine steel platens, was made. Therefore, the eccentricity along the \$y\$ axis, \$e_y\$, was calculated following the equation:

$$e_y = \frac{L \varepsilon_{SG2} - \varepsilon_{SG4}}{6 \varepsilon_{SG2} + \varepsilon_{SG4}} \quad (1)$$

where \$e_y\$ depends on the edge length \$L\$ and on the relation between the strains, measured by the strain gauges placed in two opposite cube faces, \$\varepsilon_{SG2}\$ and \$\varepsilon_{SG4}\$ in this case. Similarly, \$\varepsilon_{SG1}\$ and \$\varepsilon_{SG3}\$ were used to calculate \$e_x\$.

The eccentricity of the load caused the specimen to fail at a lower average stress than if the load was centered. This was due to the bending moment caused by the eccentric compression, which results in non-uniform stresses that can be calculated by means of the Navier equation for non-centered bending:

$$\sigma(x, y) = \frac{P}{A} + \frac{Pe_y}{I_x} y + \frac{Pe_x}{I_y} x \quad (2)$$

where \$I_x\$ and \$I_y\$ are the inertia moments of the cubic cross-section with respect to \$x\$ and \$y\$ axes, \$P\$ is the applied load, \$e_x\$ and \$e_y\$ are the load eccentricity values, and finally \$x\$ and \$y\$ are the coordinates of the point where the stress is calculated. Obviously, the stress reached its maximum value in the edge of the cube in the quadrant where the load was applied. This stress intensification encouraged the damaging processes leading to the specimen collapse to start at this most stressed zone [35].

2.4 Monotonic and fatigue tests on SFRC cubes

Firstly, in order to characterize the SFRC, monotonic compressive tests on cubic specimens were conducted, and the material compressive strength \$f_c\$ was obtained. Thirty compressive tests were performed at a loading rate of 0.3 MPa/s. They were divided in such a way that fifteen tests were performed with the i-BSJ and another fifteen without it.

Secondly, sixty specimens were tested under compressive cyclic loads. As before, half the tests were conducted with the use of the i-BSJ and the other half without it. The specimens were also divided into two series according to the following stress levels:

- 1st series: sinusoidal stress cycles varying between a minimum stress, \$\sigma_{min}\$, of \$0.24f_c\$ and a maximum stress, \$\sigma_{max}\$, of \$0.88f_c\$.
- 2nd series: sinusoidal stress cycles varying between \$0.36f_c\$ and \$0.82f_c\$.

These stress levels were chosen in order to reach a target average fatigue life of \$10^3\$ and \$10^5\$ cycles respectively according to the \$S-N\$ curves of the Model Code [10] (without accounting for the reliability analysis contained therein). It should be emphasized that the loading limits in the fatigue series performed with the i-BSJ refer to the compressive strength obtained with the special device. Thus, fifteen

specimens were tested at each combination of stress level and eccentricity condition with the loading frequency established at 10 Hz. The tests were performed following the previously-described alignment procedure. The experimental details are summarized in Table 1.

3 Results and discussion

3.1 Results of tests to characterize the load eccentricity

Figure 5 plots the stress-strain curves of two of the eccentricity characterization tests, with the i-BSJ and without it. As can be observed, the use of the i-BSJ results in almost equal maximum strains at the opposite free sides of the cube, Fig. 5b, while in the tests without it the maximum strains were uneven, see Fig. 5a.

Table 2 shows the maximum strain values during the tests performed with and without the use of the i-BSJ. The table includes the eccentricity values e_x and e_y , calculated along the x and y axes respectively (see Fig. 3) their mean values m and the invariants of their covariance matrices σ_I and σ_{II} corresponding to the 2D normal distribution of the eccentricity taken as a vector ($\mathbf{e} = e_x \mathbf{i} + e_y \mathbf{j}$).

Figures 6 and 7 plot the eccentricity results in the x - y plane for plain and i-BSJ testing conditions respectively. The contour curves in both figures correspond to equal values of the normal density function, i. e. to points with the same probability of occurrence. It should be noted that the scale in Fig. 7 is ten times larger than the scale of Fig. 6 and that the shaded area in Fig. 6 corresponds to the outer ellipse in Fig. 7. It follows that all the experimental points obtained with

Table 1 Details of the tests

Type of test	No. tests	Note	Test parameters
Monotonic	15	no i-BSJ	0.3 MPa/s
	15	i-BSJ	
Cyclic: 1 st series	15	no i-BSJ	$\sigma_{min} = 0.24f_c$; $\sigma_{max} = 0.88f_c$; $f = 10$ Hz
	15	i-BSJ	
Cyclic: 2 nd series	15	no i-BSJ	$\sigma_{min} = 0.36f_c$; $\sigma_{max} = 0.82f_c$; $f = 10$ Hz
	15	i-BSJ	

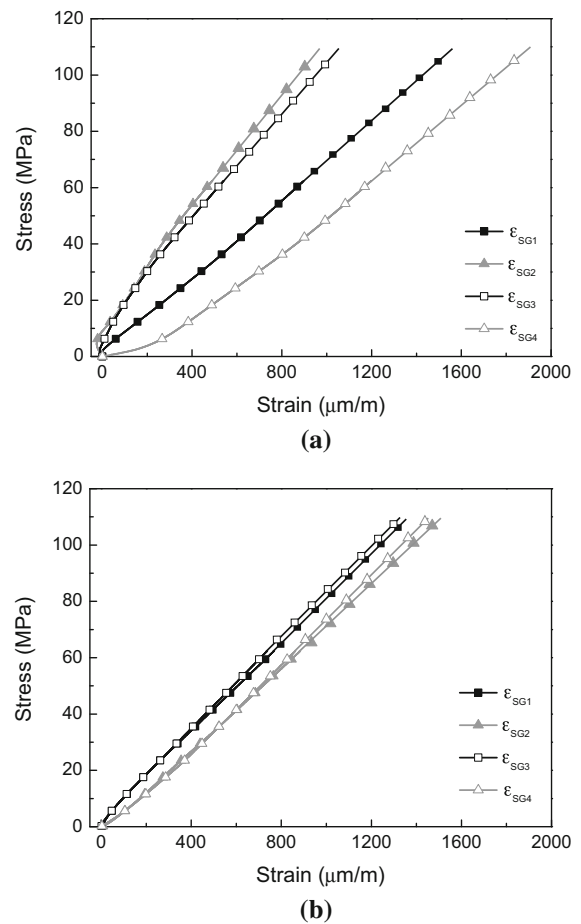


Fig. 5 Stress-strain curves without the i-BSJ (a) and with it (b)

the i-BSJ fall in an area that is significantly smaller than the region with the same probability of containing the experimental points for the plain tests. Besides, note that the contour curves are closer to each other in the i-BSJ case, which means that the density surface is steeper and thus the experimental points have less relative scatter.

These same ideas can be drawn from the comparison of the invariants of the covariance matrix of the normal 2D density function (σ_I and σ_{II}) for the two cases, which are 2.70 mm and 1.14 mm² for the plain case and 0.20 mm and 0.65 × 10⁻² mm² for the i-BSJ eccentricity values. Indeed, the invariants obtained with the i-BSJ are one and two orders of magnitude lower (for σ_I and σ_{II} respectively) than the corresponding ones from the plain tests. Interestingly, the mean eccentricity values of the two distributions are quite close, as can be seen in Figs. 6 and 7. They are

Table 2 Strain and eccentricity values at 110 MPa on the aluminum cube with and without the use of the i-BSJ

Test no	ε_{SG1} ($\mu\text{m}/\text{m}$)	ε_{SG3} ($\mu\text{m}/\text{m}$)	e_x (mm)	ε_{SG2} ($\mu\text{m}/\text{m}$)	ε_{SG4} ($\mu\text{m}/\text{m}$)	e_y (mm)
1	1451	1107	0.90	1193	1661	- 1.09
2	947	1604	- 1.72	1563	1327	0.54
3	1377	1028	0.97	1517	1223	0.72
4	1189	1511	- 0.80	1696	943	1.90
5	1452	1039	1.11	1335	1615	- 0.63
6	1273	1468	- 0.47	1622	992	1.61
7	1800	1514	0.58	1339	974	1.05
8	1914	748	2.92	1043	1814	- 1.80
9	1781	1301	1.04	1132	1583	- 1.11
10	1685	725	2.66	1215	1733	- 1.17
11	1546	1299	0.58	1332	1411	- 0.19
12	1282	1332	- 0.13	1287	1555	- 0.63
13	1540	1162	0.93	1344	1327	0.04
14	1542	995	1.44	1645	1184	1.09
15	1464	1310	0.37	1221	1544	- 0.78
Mean	—	—	0.69	—	—	- 0.03

Invariants of the covariance matrix: $\sigma_I = 2.70 \text{ mm}$ and $\sigma_{II} = 1.14 \text{ mm}^2$

Test i-BSJ	ε_{SG1} ($\mu\text{m}/\text{m}$)	ε_{SG3} ($\mu\text{m}/\text{m}$)	e_x (mm)	ε_{SG2} ($\mu\text{m}/\text{m}$)	ε_{SG4} ($\mu\text{m}/\text{m}$)	e_y (mm)
1	1422	1310	0.27	1431	1275	0.38
2	1420	1305	0.28	1416	1278	0.34
3	1432	1289	0.35	1427	1274	0.38
4	1425	1317	0.26	1414	1323	0.22
5	1418	1328	0.22	1429	1299	0.32
6	1429	1309	0.29	1400	1314	0.21
7	1403	1312	0.22	1369	1332	0.09
8	1423	1313	0.27	1388	1318	0.17
9	1451	1289	0.39	1401	1324	0.19
10	1419	1333	0.21	1356	1367	-0.03
11	1450	1334	0.28	1390	1306	0.21
12	1428	1313	0.28	1373	1343	0.07
13	1461	1293	0.41	1381	1322	0.15
14	1418	1324	0.23	1369	1359	0.02
15	1437	1273	0.40	1395	1321	0.18
Mean	—	—	0.29	—	—	0.19

Invariants of the covariance matrix: $\sigma_I = 0.20 \text{ mm}$ and $\sigma_{II} = 0.65 \times 10^{-2} \text{ mm}^2$

plotted as hollow squares in both figures and it is clear that they are quite close to each other.

The points and the contour plots in Fig. 7 indicate that there is a systematic error in the alignment of the load of the system formed by the i-BSJ and the aluminum cube. However, this error is quite small since the mean value of the eccentricity is only 0.35 mm

apart from the geometrical center, roughly 0.9% of the edge of the cube. Besides, the area where all the results fall is quite small, as can be seen in the two figures (and it is also indicated by the low values of the invariants of the covariance matrix). This small error is a consequence of the tolerances in the fabrication of the several pieces involved (aluminum cube, plates of



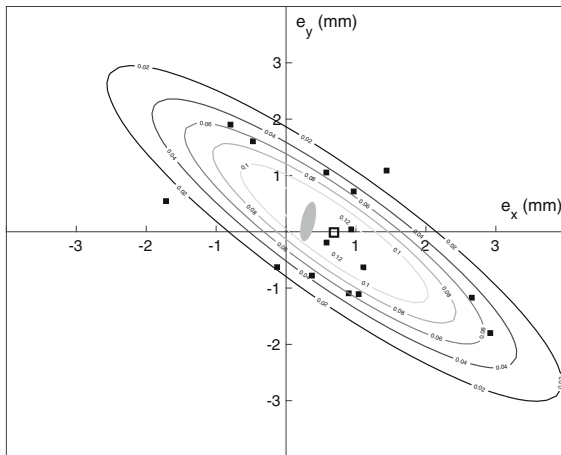


Fig. 6 Load eccentricity without the i-BSJ

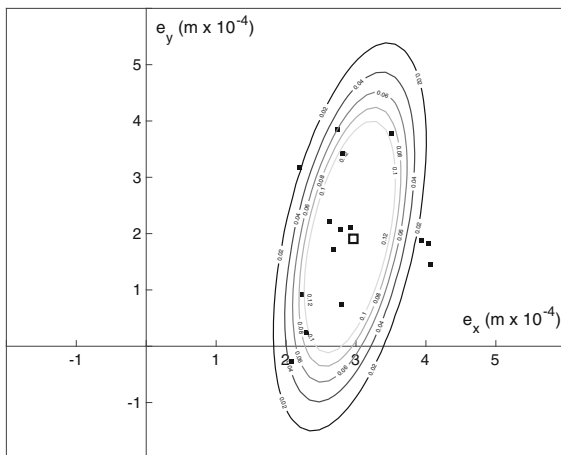


Fig. 7 Load eccentricity with the i-BSJ

Table 3 Material properties

Material	No. of tests	ρ (kg/m ³)	f_c (MPa)	Note
SFRC	15	2334 (23)	53.6 (5)	no i-BSJ
	15		58.9 (3)	i-BSJ

the i-BSJ, location and radius of the recesses etc) and cannot be avoided.

The comparison between Figs. 6 and 7 demonstrates that the use of the i-BSJ significantly reduced the uncertainty on load position. Therefore, the use of the i-BSJ minimizes the undesired eccentricity variation due to manual specimen centering. The eccentricities resulting from the tests with the i-BSJ are due to

tolerances in the device and in the geometry of the specimen.

3.2 Results of monotonic and fatigue tests on SFRC cubes

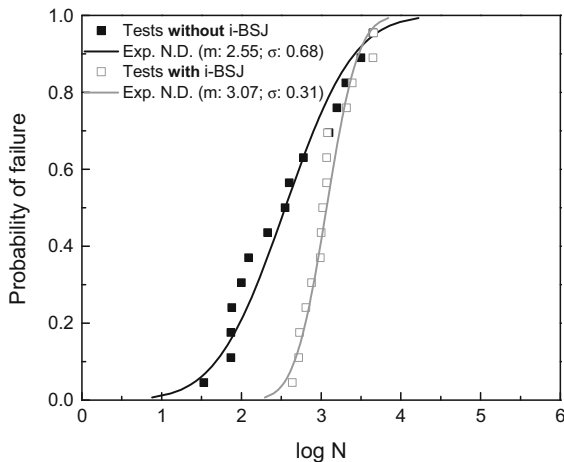
Prior to conducting fatigue tests on SFRC specimens, the compressive strength f_c of the material was needed in order to set the fatigue stress levels for the 1st and 2nd series of tests. Thereby, a total of thirty compressive characterization tests were performed in accordance with the previously-described alignment procedure. The tests were carried out with and without the use of the i-BSJ. The test results are shown in Table 3. The figures in parentheses are the standard deviations. Therefore, the use of the i-BSJ increased the obtained compressive strength f_c of the SFRC material by 10% and reduced its scatter, thereby bringing it closer to the real material property [35]. The use of the i-BSJ flattened the stress profile at the specimen section and delayed the formation of the cracking and damage processes, which resulted in a greater compressive strength.

The fatigue test results of SFRC specimens, with and without the use of the i-BSJ are shown in Table 4 for the stress level corresponding to the 1st and 2nd series of tests. Figure 8 plots the fatigue life, expressed as the decimal logarithm of the number of resisted cycles, $\log N$, versus the probability of failure for the 1st series of fatigue tests. The solid squares represent the results of tests done without the i-BSJ whereas the empty ones correspond to the fatigue lives obtained with the device. The normal distribution function that corresponds to each type of tests is also plotted. Similarly, Fig. 9 shows the experimental number of cycles for the 2nd series of tests and the corresponding distributions for the probability of failure.

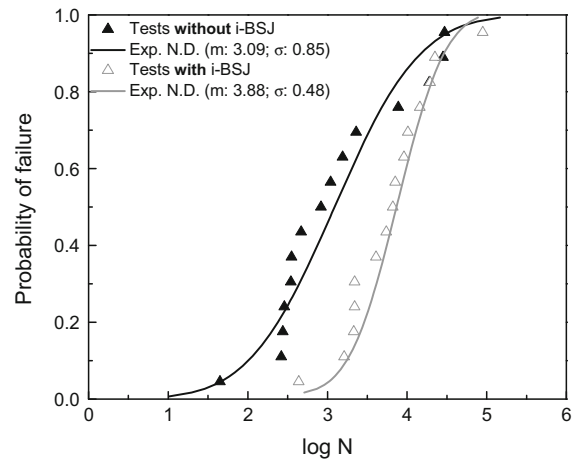
The average number of cycles until failure increased with the use of the i-BSJ for the two series of fatigue tests. Specifically, the average fatigue life tripled for the 1st series of tests, from 355 to 1175 cycles (2.55 to 3.07 in terms of $\log N$). Incidentally, note that the 10^3 cycle target was fairly achieved in reality, Fig. 8, while it was six times greater for the 2nd series, increasing from 1230 to 7586 cycles (3.09 to 3.88 in terms of $\log N$, this time below the 10^5

Table 4 Cycles resisted by the SFRC

1 st series: $\sigma_{min} = 0.24 f_c$ and $\sigma_{max} = 0.88 f_c$					
N					Note
100	74	213	75	3129	no i-BSJ
1261	1571	4488	2057	606	
401	353	122	34	74	
434	1042	4563	519	4426	i-BSJ
1178	2471	2071	765	1186	
646	992	973	541	1203	
2 nd series: $\sigma_{min} = 0.36 f_c$ and $\sigma_{max} = 0.82 f_c$					
N					Note
353	7756	29176	28214	1548	no i-BSJ
463	45	346	835	19037	
2313	266	274	291	1085	
14429	19345	2209	2157	6655	i-BSJ
88758	1609	5519	9177	10227	
2179	22499	4048	7113	16600	

**Fig. 8** Fatigue life for the 1st series of tests ($\sigma_{min} = 0.24f_c$ and $\sigma_{max} = 0.88f_c$) with and without the i-BSJ

cycles target from the $S-N$ curves of the Model Code), Fig. 9. Furthermore, the standard deviation of the tests was halved with the use of the i-BSJ. It decreased by 55%, from 0.68 to 0.31 for the 1st series of tests and by 43% for the 2nd series, from 0.85 to 0.48. However, the absolute values of the deviation are greater for the tests of the 2nd series, therefore the slope of the probability of failure curve is flatter than those of the 1st series. This corroborates previous observations indicating that stress levels leading to long lives had greater deviations than those leading to fewer cycles until failure [3]. Moreover, it should be noted that the enhancement in fatigue life achieved by minimizing

**Fig. 9** Fatigue life for the 2nd series of tests ($\sigma_{min} = 0.36f_c$ and $\sigma_{max} = 0.82f_c$) with and without the i-BSJ

unwanted loading eccentricity was obtained in spite of the fact that stress levels refer to f_c from monotonic tests with the i-BSJ. If the reference f_c obtained without the i-BSJ had also been used for the tests with the device (which could be considered correct since the material is always the same), the target values given by the $S-N$ curves of the Model Code [10] would have been $10^{4.5}$ and $10^{6.4}$ for the 1st and 2nd series respectively (instead of 10^3 and 10^5).

The results in Figs. 8 and 9 also demonstrate the influence of undesired eccentricity on the scatter of the results. The scatter is not only represented by the standard deviation of the failure distribution, but also by the width of the spindle-shaped region between the distributions obtained with and without the i-BSJ, which could have been even wider in the event that the reference strength had been kept constant for all the tests. The two series of tests performed with the i-BSJ may be viewed as the limit case of no or very low loading eccentricity for these particular loading levels. Eccentric cyclic loads lead to shorter fatigue lives, i. e. to distributions on the left of the limit curve. The more eccentricity, the farther the results will be from the limit curve. The less eccentricity, the closer to the limit curve. The curves seem indeed to converge for long lives. In addition, note that the deviation of the results reduces with the i-BSJ, but it is still quite large, which indicates that there are other sources of uncertainty that have not been eliminated, mainly the material heterogeneity.

It should be noted that the loading eccentricity may not be constant during a single fatigue test. As the load is cyclic, there may be also a movement of the load axis during the cycle. The length of this movement can be estimated by assuming that the strain at the cube faces would correspond to the curves in Fig. 5. As an example, we can evaluate the eccentricity variation for the cycles that correspond to the first series. The stress span goes from $0.24 f_c$ to $0.88 f_c$ and, so, in the tests without the i-BSJ it goes from 12.9 to 47.2 MPa, whereas in the i-BSJ case the stresses go from 14.1 to 51.8 MPa. Making the corresponding readings and calculations, we get that the eccentricity varies between $\mathbf{e}_1 = 3.45 \mathbf{i} - 5.41 \mathbf{j}$ mm and $\mathbf{e}_2 = 1.96 \mathbf{i} - 3.28 \mathbf{j}$ mm for the plain case (the increment of the eccentricity is $\mathbf{e}_2 - \mathbf{e}_1$ which implies that the load moves a distance of 2.60 mm between the two points; note that the load gets closer to the origin as it increases) and between $0.03 \mathbf{i} - 0.02 \mathbf{j}$ mm and $0.11 \mathbf{i} + 0.03 \mathbf{j}$ mm for the i-BSJ case (the movement is of only 0.09 mm). It follows that, for this particular example, the length of the load movement for the plain test is almost 30 times bigger than that of the i-BSJ case.

As for the reasons behind the damaging effect of eccentric loading, eccentricity causes the stresses to lose uniformity and to achieve damage localization faster, which results in shorter fatigue lives. Therefore, the longer the load eccentricity is, the shorter fatigue life we obtain. It is clear that the use of the i-BSJ improves the results by increasing the resulting compressive strength in monotonic tests and by increasing fatigue life and reducing the deviations and the scatter. Thus, the use of an i-BSJ is highly recommended for laboratory compressive monotonic and fatigue tests in order to minimize or eliminate the uncertainty caused by loading eccentricity.

4 Conclusions

The effect of the uncertainty on load position in the fatigue life of SFRC and its scatter was revealed in this paper. An individualized ball-and-socket joint (i-BSJ) was designed in order to minimize the unwanted loading eccentricity. Subsequently, two types of tests were performed. On the one hand, an instrumented aluminum cube was used to determine the eccentricity under two testing conditions, that is with and without

the i-BSJ. On the other hand, two series of 15 monotonic compressive tests and two series of 15 cyclic compressive tests were performed on 40 mm edge-length SFRC cubes, again with and without the special device.

The results demonstrate that, although the average eccentricity values did not change significantly, their standard deviation was one order of magnitude less with the new device. This means that the load eccentricity caused by misalignments due to manual specimen centering and by geometrical relations between the spherical seat of the press and the specimen is significantly reduced, but the effect of tolerances on experimental equipment and specimen geometry remained. Moreover, the use of the i-BSJ on the tests of SFRC cubes produced an increase of 10% in the average f_c , whereas the average fatigue life tripled for the first series and was six times longer for the second series, notwithstanding the loading limits in the low-eccentricity series, referred to as the enhanced f_c . Similarly, the standard deviation of the number of cycles until failure decreased in both i-BSJ fatigue series. Therefore, undesired loading eccentricity shortens fatigue lives and increases scatter in the results, which cannot only be attributed to variations in the compressive strength [26–28].

Finally, the use of an i-BSJ is highly recommended in order to eliminate the uncertainty caused by misalignments due to manual specimen centering, both in monotonic and cyclic compressive tests.

Acknowledgements The authors acknowledge the financial support from the *Ministerio de Economía y Competitividad*, Grant BIA2015-68678-C2-R, Spain, and from *Consejería de Educación, Cultura y Deportes, Junta de Comunidades de Castilla-La Mancha, Spain, & Fondo Europeo de Desarrollo Regional*, Grant PEII-2014-016-P and INCRECYT Program.

Compliance with ethical standards

Conflict of interest The authors declare that they have no conflict of interest.

References

1. ASTM C39/C39M (2015) Standard test method for compressive strength of cylindrical concrete specimens. ASTM International, West Conshohocken, Pennsylvania
2. EN 12390-13 (2014) Testing hardened concrete—Part 13: determination of secant modulus of elasticity in compression. EN European standards



3. CEB 188. Comité Euro-International du Béton (1988) Fatigue of concrete structures: state of the art report. Bulletin d'Information no 188, Lausanne
4. ACI 215R-74 [Revised 1992/Reapproved 1997] (2001) Considerations for design of concrete structures subjected to fatigue loading. ACI manual of concrete practice, part 1, American Concrete Institute, Farmington Hills, Michigan
5. Susmel L (2014) A unifying methodology to design unnotched plain and short-fibre/particle reinforced concretes against fatigue. *Int J Fatigue* 61:226–243
6. Zanuy C, Albajar L, de la Fuente P (2011) The fatigue process of concrete and its structural influence. *Mater Const* 61:385–399
7. Saucedo L, Yu RC, Medeiros A, Zhang XX, Ruiz G (2013) A probabilistic fatigue model based on the initial distribution to consider frequency effect in plain and fiber reinforced concrete. *Int J Fatigue* 48:308–318
8. Ríos JD, Cifuentes H, Yu RC, Ruiz G (2017) Probabilistic flexural fatigue in plain and fiber-reinforced concrete. *Materials* 10(767):1–25
9. Eurocode 2 (2008) Design of concrete structures. european committee for standardization. EN 1992-2:2005/AC:2008. European Standards
10. Model Code 2010; Final draft (2012) fib Bulletin no 65 and 66, EPFL Lausanne
11. Graf O, Brenner E (1934) Experiments for investigating the resistance of concrete under repeated compression loads. Deutscher Ausschuss für Eisenbeton, Bulletin no 76 (**in German**)
12. Graf O, Brenner E (1936) Experiments for investigating the resistance of concrete under repeated compression loads 2. Deutscher Ausschuss für Eisenbeton, Bulletin no 83 (**in German**)
13. Kesler CE (1953) Effect of speed of testing on flexural fatigue strength of plain concrete. *HRB Proc* 32(5):251–258
14. Sparks PR, Menzies JB (1973) Effect of rate of loading upon the static and fatigue strengths of plain concrete in compression. *Mag Concr Res* 25(83):73–80
15. Hsu TTC (1981) Fatigue of plain concrete. *J Am Concr Inst* 78(4):292–305
16. Hwan OhB (1986) Fatigue analysis of plain concrete in flexure. *J Struct Eng* 112(2):273–288
17. Hwan OhB (1991) Fatigue-life distributions of concrete for various stress levels. *ACI Mater J* 88(2):122–128
18. Zhang B, Phillips DV, Wu K (1996) Effects of loading frequency and stress reversal on fatigue life of plain concrete. *Mag Concr Res* 48(4):361–375
19. Medeiros A, Zhang XX, Ruiz G, Yu RC, Velasco MDSL (2015) Effect of the loading frequency on the compressive fatigue behavior of plain and fiber reinforced concrete. *Int J Fatigue* 70:342–350
20. Aas Jakobsen K (1970) Fatigue of concrete beams and columns. Bulletin no 70-1, University of Trondheim. Norwegian Institute of Technology. Division of Concrete Structures, Trondheim
21. Tepfers R, Kutti T (1979) Fatigue strength of plain, ordinary and lightweight concrete. *ACI J* 76(5):635–652
22. Tepfers R (1979) Tensile fatigue strength of plain concrete. *ACI J* 76(8):919–933
23. Hilsdorf HK, Müller HS (1999) Concrete. Structural concrete, CEB/FIB manual textbook: textbook on behaviour. *Des Perform* 1:21–83
24. Waagaard K, Keep B, Stemland H (1987) Fatigue of high strength lightweight aggregate concrete. In: Proceedings of utilization of high strength concrete, Stavanger
25. Petkovic G, Lenchow R, Stemland H, Rosseland S (1990) Fatigue of high strength concrete. In: Proceedings of the second international symposium on application of high strength concrete, Berkeley
26. Holmen JO (1979) Fatigue of concrete by constant and variable amplitude of loading. Ph.D. thesis, Division of Concrete Structures, The Norwegian Institute of Technology, The University of Trondheim
27. Siemes AJM (1983) Fatigue of concrete, part 1: compressive stresses (in Dutch with extended English summary). IRO-MATS/CUR report no 112
28. Cachim PB, Figueiras JA, Pereira PAA (2002) Fatigue behavior of fiber-reinforced concrete in compression. *Cement Concr Compos* 24(2):211–217
29. EN 12390-3 (2009) Testing hardened concrete—part 3: compressive strength of test specimens. EN European Standards
30. Ople FS, Hulsbos CL (1966) Probable fatigue life of plain concrete with stress gradient. In: ACI proceedings, vol. 63, pp 59–82, Publication no 295, Fritz laboratory reports. Paper 1534
31. Mindess S, Young JF, Darwin D (2003) Concrete, 2nd edn. Prentice Hall, Pearson Education Inc., Upper Saddle River
32. Poveda E, Ruiz G, Cifuentes H, Yu RC, Zhang XX (2017) Influence of the fiber content on the compressive low-cycle fatigue behavior of self-compacting SFRC. *Int J Fatigue* 101:9–17
33. Ponikiewski T, Golaszewski J (2013) Properties of steel fibre reinforced self-compacting concrete for optimal rheological and mechanical properties in precast beams. *Proc Eng* 65:290–295
34. Bentur A, Mindess S (2007) Fibre reinforced cementitious composites. Taylor and Francis, London
35. del Viso JR, Carmona JR, Ruiz G (2008) Shape and size effects on the compressive strength of high-strength concrete. *Cement Concr Res* 38:386–395

